Brain Stimulation 10 (2017) 46–50

Contents lists available at ScienceDirect

Brain Stimulation

journal homepage: www.brainstimjrnl.com

Role of Soft-Tissue Heterogeneity in Computational Models of Deep Brain Stimulation

Bryan Howell, Cameron C. McIntyre *

Department of Biomedical Engineering, Case Western Reserve University, Cleveland, OH, USA

ARTICLE INFO

Article history:
Received 25 April 2016
Received in revised form 29 August 2016
Accepted 5 September 2016
Available online 8 September 2016

Keywords:
Deep brain stimulation
Electric field
Heterogeneity
Vasculature
Soft tissues

ABSTRACT

Background: Bioelectric field models of deep brain stimulation (DBS) are commonly utilized in research and industrial applications. However, the wide range of different representations used for the human head in these models may be responsible for substantial variance in the stimulation predictions.
Objective: Determine the relative error of ignoring cerebral vasculature and soft-tissue heterogeneity outside of the brain in computational models of DBS.
Methods: We used a detailed atlas of the human head, coupled to magnetic resonance imaging data, to construct a range of subthalamic DBS volume conductor models. We incrementally simplified the most detailed base model and quantified changes in the stimulation thresholds for direct activation of corticofugal axons.
Results: Ignoring cerebral vasculature altered predictions of stimulation thresholds by <10%, whereas ignoring soft-tissue heterogeneity outside of the brain altered predictions between –44 % and 174%.
Conclusions: Heterogeneity in the soft tissues of the head, if unaccounted for, introduces a degree of uncertainty in predicting electrical stimulation of neural elements that is not negligible and thereby warrants consideration in future modeling studies.

Introduction

Magnetic resonance image (MRI)-based bioelectric field models of the human head show promise for optimizing deep brain stimulation (DBS) therapies [1]. These models typically use finite element methods to solve for the electric field generated during DBS and are coupled to cable models of axons to quantify the neural response to stimulation. However, a wide range of different model representations for the human head are currently used in both academic and industrial research. We hypothesized that these volume conductor differences are responsible for substantial variance in model predictions.

Recent studies have identified the degree of heterogeneity and anisotropy that is required to accurately model the electric field in the human head [2], while others have highlighted the importance of accurately representing boundary conditions in models of DBS [3,4]. Therefore, the goal of this study was to integrate the latest advancements in anatomical and electrical DBS modeling to identify the role of cerebral vasculature and soft-tissue heterogeneity outside the brain on the neural response to stimulation. We used a highly detailed multimodal image-based anatomical model of a human head and neck, or MIDA, which was recently made available by the FDA [5], as a template for constructing a range of subthalamic DBS models. The degree of model detail ranged from complex to simple and enabled us to quantify errors in predicting the neural response to DBS that are associated with ignoring cerebral vasculature and soft-tissue heterogeneity outside the brain.

Materials and methods

The methodology in this study was adopted from our previous work [2] with specific integration of the MIDA atlas volumes [5].

Image processing

All images, unless specified otherwise, were processed using the FMRIB software library (FSL) v5.1 [6]. MIDA contains locations of 116 anatomical structures [5]. Our base case, $MIDA_{12}$, was constructed by combing the 116 structures into 12 electrically equivalent classifications: dura, grey matter, white matter, CSF, muscle, tendon, bone, fat, dry skin, intervertebral disks, blood, and air. Subsequently, these 12 regions were combined in different ways to form four simplified anatomical representations: $MIDA_{11}$, $MIDA_{7}$, $MIDA_{6}$,

* Corresponding author.
E-mail address: ccm4@case.edu (C.C. McIntyre).

1935-861X/
http://dx.doi.org/10.1016/j.brs.2016.09.001

and $MIDA_1$ (Fig. 1a). $MIDA_{11}$ was derived from $MIDA_{12}$ by substituting the voxels of blood with the mode type of tissue across the 26 nearest neighbors, with replacement. If the mode was blood, the voxel of blood was replaced by the majority constituent, which was grey matter and muscle inside and outside the brain, respectively. $MIDA_7$ and $MIDA_6$ were derived from $MIDA_{12}$ and $MIDA_{11}$, respectively, by constructing a partial skull that enclosed the brain and combining all other regions outside the skull into a lumped soft-tissue region. We constructed the partial skull by dilating the brain mask and subtracting the dilated and original masks so that the resultant shell was contained within but not outside the portion of the skull that surrounded the brain. We constructed $MIDA_1$ by treating the entire head as a homogeneous, isotropic conductive medium, except for the encapsulation sheath (see below).

The MR images used to construct MIDA are not publically available. Therefore, we co-registered MIDA to the MNI 152 standard space using a 12-parameter affine transformation. The inverse transformation was used to map a probabilistic atlas of a subthalamic nucleus (STN) [7] from MNI space to MIDA. We thresholded the atlas so that the volume of the STN was ~150 mm^3 [8]. We also used a 12-parameter affine transformation to co-register MIDA to the diffusion-weighted (DW) MR image of the healthy subject from FSL's course data. The DW image, which underwent eddy-current and susceptibility corrections, was used to help define anisotropy within the brain.

Bioelectric field models

We constructed five bioelectric field models corresponding to the five different anatomical representations that we derived from MIDA. We used Seg3D [9] to construct tessellated surfaces that bounded the brain, skull, and soft-tissue volumes of $MIDA_{7/6}$. Next, we modeled the Medtronic 3389 DBS electrode array, placed it within the right STN (Fig. 1b), and enclosed it by a 0.5 mm thick layer of encapsulation tissue [10,11]. Finally, we used COMSOL Multiphysics v5.1 (COMSOL Inc., Burlington, MA) to construct tetrahedral meshes within the aforementioned volumes. The union of all three meshes was the tetrahedral mesh used for all five head models.

For each head model, the corresponding anatomical representation was used to help define a conductivity tensor (Σ) for all elements comprising the tetrahedral mesh. Anatomical representations originally derived from MIDA had voxels that were 0.5 mm × 0.5 mm × 0.5 mm, but due to memory constraints in defining the tensor field, we down-sampled the images to 1 mm × 2 mm × 2 mm. Σs within the parenchyma and CSF of the brain were modeled as anisotropic. The eigenvectors of these Σs were derived from the fitted diffusion tensors of the DW MR image, and the load preservation approach from [2] was used to calculate eigenvalues of Σ given an isotropic conductivity (σ) and eigenvalues of the diffusion tensors. Σs in all other regions, including the encapsulation tissue, were isotropic. That is, $\Sigma = \sigma I$, where I is the identify matrix. The σs for each tissue type were the measured conductivities from [12] at 1 kHz. The exceptions were the encapsulation, dura and air, which had a σ of 0.13 S/m [13], 0.03 S/m [14], and 1×10^{-12} S/m, respectively. The σ of the homogeneous isotropic regions in $MIDA_7$, $MIDA_6$, and $MIDA_1$ were chosen so that the electrical load of contact 2 matched that of $MIDA_{12}$ (precision <0.1 %). The electrical load was the access resistance of the electrode plus the dynamic load of the electrode-tissue interface (see below) at the end of a 70 µs stimulus pulse, thereby matching the calculation of Medtronic IPGs.

We used the finite element method to solve Laplace's equation for monopolar and bipolar electrode configurations. In the monopolar case, electrode 2 was the cathode, and the outer boundary of the head was insulated, except at the base of the neck, which was set

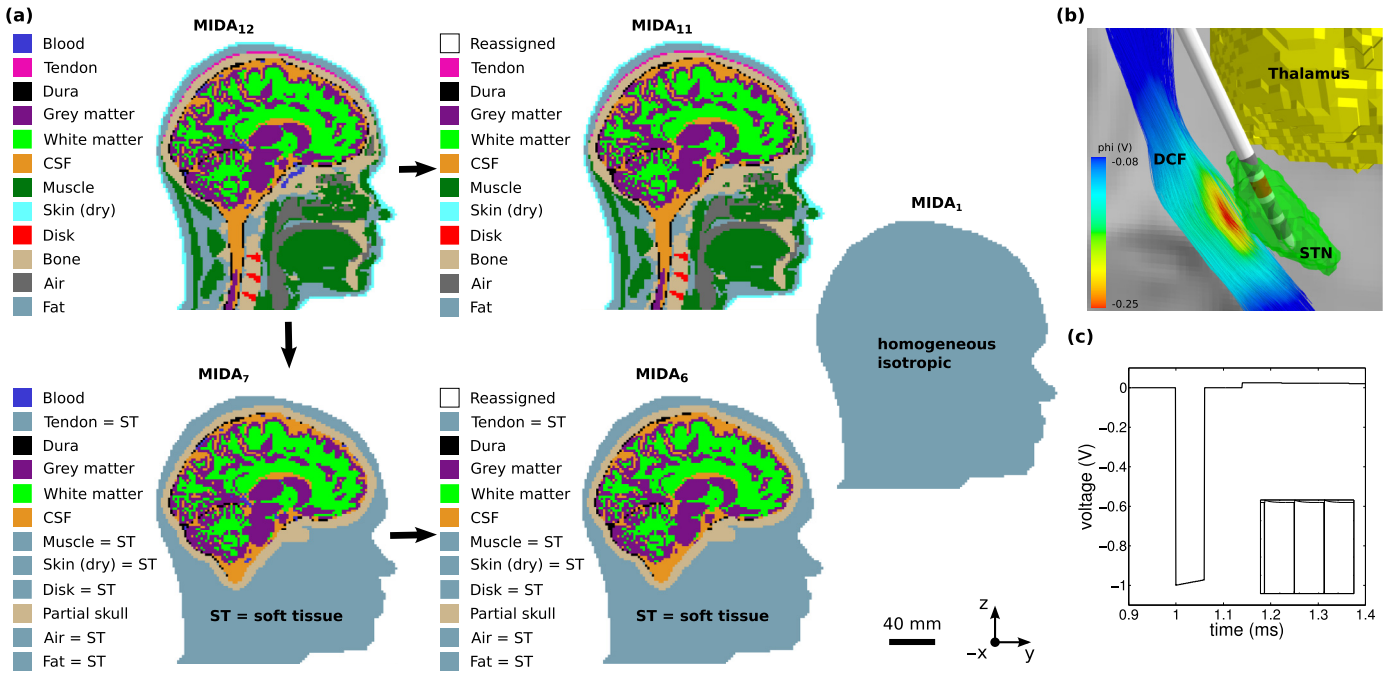

Figure 1. Models of subthalamic DBS. (a) Computational models were derived from five electrical representations of MIDA [5] (sagittal views). $MIDA_{12}$ is MIDA combined into 12 electrically equivalent classifications. $MIDA_{11}$ is $MIDA_{12}$ but without blood (see *Image Processing*). $MIDA_7$ and $MIDA_6$ were derived from $MIDA_{12}$ and $MIDA_{11}$, respectively, by combining six regions and portions of the skull into a single soft-tissue (ST) region. $MIDA_1$ was constructed by treating the entire head, as a homogeneous and isotropic medium. (b) The Medtronic 3339 lead was implanted in the subthalamic nucleus (STN) and used to stimulate descending corticofugal (DCF) axons. A 0.5 mm thick encapsulation sheath surrounded the lead. The applied potentials reflect monopolar cathodic stimulation at an amplitude of –1 V. (c) The voltage drop across the electrical load of the head over time. Inset shows three pulses delivered at 130 Hz.